RESEARCH ARTICLE

Inducible Activation of MyD88 and CD40 in CAR T Cells Results in Controllable and Potent Antitumor Activity in Preclinical Solid Tumor Models

Melinda Mata[1,2,3], Claudia Gerken[1,2,3], Phuong Nguyen[1,2,3], Giedre Krenciute[1,2,3], David M. Spencer[4,5], and Stephen Gottschalk[1,2,3,4]

ABSTRACT Adoptive immunotherapy with T cells expressing chimeric antigen receptors (CAR) has had limited success for solid tumors in early-phase clinical studies. We reasoned that introducing into CAR T cells an inducible costimulatory (iCO) molecule consisting of a chemical inducer of dimerization (CID)–binding domain and the MyD88 and CD40 signaling domains would improve and control CAR T-cell activation. In the presence of CID, T cells expressing HER2–CARζ and a MyD88/CD40–based iCO molecule (HER2ζ.iCO T cells) had superior T-cell proliferation, cytokine production, and ability to sequentially kill targets *in vitro* relative to HER2ζ.iCO T cells without CID and T cells expressing HER2–CAR.CD28ζ. HER2ζ.iCO T cells with CID also significantly improved survival *in vivo* in two xenograft models. Repeat injections of CID were able to further increase the antitumor activity of HER2ζ.iCO T cells *in vivo*. Thus, expressing MyD88/CD40–based iCO molecules in CAR T cells has the potential to improve the efficacy of CAR T-cell therapy approaches for solid tumors.

SIGNIFICANCE: Inducible activation of MyD88 and CD40 in CAR T cells with a small-molecule drug not only enhances their effector function, resulting in potent antitumor activity in preclinical solid tumors, but also enables their remote control post infusion. *Cancer Discov; 7(11); 1306–19. ©2017 AACR.*

INTRODUCTION

Chimeric antigen receptors (CAR) are engineered fusion proteins that couple the antigen recognition capability of an antibody with the effector function of a T cell, thereby directing T-cell specificity toward tumor cells in an MHC-independent manner. Despite the remarkable and durable antitumor effects of CAR T cells for CD19-positive malignancies, the adoptive transfer of CAR T cells to treat solid tumors has had limited clinical success so far (1, 2). Several factors likely contribute to the diminished function of CAR T cells in the context of solid tumors, including insufficient homing of infused T cells to tumor sites or their reduced function within the immunosuppressive tumor microenvironment (3–5). Combined with "on-target, off-tumor" safety concerns (6, 7), a strategy to selectively modulate CAR T-cell function *in vivo* would be ideal to enhance their antitumor activity.

Inducible systems to regulate gene expression or turn on signaling pathways are an attractive approach to control activation and function of immune cells. For example, early-phase clinical studies have shown that T cells genetically modified to express an inducible caspase-9 (iC9) suicide gene encoding one $FKBP12_{v36}$ chemical inducer of dimerization (CID)–binding domain linked to caspase recruitment domain (CARD)–deleted C9 can be ablated with a small-molecule ligand (AP1903; ref. 8).

$FKBP12_{v36}$-based molecules have also been developed to activate immune cells. For example, dendritic cells expressing a molecule consisting of a myristoylation-targeting sequence, MyD88 lacking its TIR domain, the cytoplasmic domain of CD40, and two tandem $FKBP12_{v36}$ domains (iMyD88.CD40) can be activated *in vivo* with CID resulting in potent antitumor activity (9). Although CD28 is the canonical costimulatory signal for T-cell activation, Toll-like receptors (TLR) are also expressed in activated T cells and provide costimulation (10). Downstream TLR signaling involving MyD88 activates NF-κB and PI3K/AKT signaling and enhances effector function, particularly of tumor-specific T cells (11–13). Likewise, CD40, a cell-surface receptor mainly expressed on antigen-presenting cells (APC), is also expressed on T cells and plays an intrinsic role in T-cell costimulation, differentiation, memory formation, and rescue from exhaustion (14–17).

To explore whether inducible MyD88 and CD40 signaling could be utilized to enhance CAR T-cell function, we constructed a panel of inducible costimulatory (iCO) molecules. Here, we demonstrate that CAR T cells expressing iMyD88.CD40 had superior effector function in the presence of CID *in vitro* and *in vivo* in two xenograft mouse models compared with our clinically validated HER2.CD28ζ T cells (18).

RESULTS

Inducible Activation of MyD88 and CD40 in T Cells Is Required for Optimal IL2 Production after CD3ζ Stimulation

We synthesized a panel of iCO mini-genes to investigate whether activation of MyD88 and CD40 signaling pathways is required for optimal cytokine production in T cells. iCO molecules encoded a myristoylation-targeting sequence, MyD88 ± TIR domain, and/or CD40, two $FKBP12_{v36}$ domains, and

[1]Center for Cell and Gene Therapy, Texas Children's Hospital, Houston Methodist Hospital, Baylor College of Medicine, Houston, Texas. [2]Texas Children's Cancer Center, Texas Children's Hospital, Baylor College of Medicine, Houston, Texas. [3]Department of Pediatrics, Baylor College of Medicine, Houston, Texas. [4]Department of Pathology and Immunology, Baylor College of Medicine, Houston, Texas. [5]Bellicum Pharmaceuticals, Houston, Texas.

Note: Supplementary data for this article are available at Cancer Discovery Online (http://cancerdiscovery.aacrjournals.org/).

Corresponding Author: Stephen Gottschalk, Baylor College of Medicine, 1102 Bates Street, Suite 1770, Houston, TX 77030. Phone: 832-824-4179; Fax: 832-825-4732; E-mail: stephen.gottschalk@stjude.org

doi: 10.1158/2159-8290.CD-17-0263

an HA-epitope [iMyD88.CD40, iMyD88TIR.CD40, iMyD88 (n-terminal $FKBP12_{v36}$ domains), iMyD88cc (c-terminal $FKBP12_{v36}$ domains), or iCD40; Supplementary Fig. S1A]. Mini-genes were subcloned into a retroviral vector upstream of an internal ribosome entry site (IRES) and mOrange. T cells expressing iCO molecules were successfully generated by retroviral transduction as judged by FACS analysis for mOrange and Western blot analysis using an HA antibody (Supplementary Fig. S1B and S1C). To assess the functionality of the iCO molecules generated, we first analyzed NF-κB pathway activation. Transduced and nontransduced (NT) T cells were activated with OKT3 ± CID, and after 30 minutes, the presence of phosphorylated IκB kinase (IKK) was determined by Western blot analysis. OKT3 induced phosphorylation of IKK in transduced and NT T cells, which was augmented by CID in transduced T cells, indicating that the generated iCO molecules are functional (Supplementary Fig. S1D).

We next determined whether activating MyD88 and CD40 signaling pathways in T cells after OKT3 stimulation enhanced cytokine production, focusing on Th1 (IFNγ, GM-CSF, TNFα, IL2) and Th2 (IL4, IL5, IL6, IL10, IL13) cytokines. In NT T cells, OKT3 stimulation ± CID induced high levels of IFNγ, TNFα, and IL13 (>1,000 pg/mL), intermediate levels of IL10 and IL5 (100 to 1,000 pg/mL), and low levels of IL2, IL6, IL4, and GM-CSF (10–100 pg/mL; Supplementary Fig. S2). OKT3 stimulation of iMyD88.CD40 T cells + CID induced an 89-fold increase in IL2, a 49-fold increase in IL6, and <5-fold increase in all other cytokines analyzed compared with OKT3-stimulated cells (Fig. 1A). This cytokine production pattern was similar for T cells expressing other MyD88-containing iCO molecules + CID; however, the fold of IL2 induction was lower (iMyD88TIR.CD40, 15-fold; iMyD88, 32-fold; iMyD88CC, 7-fold; Fig. 1A; Supplementary Fig. S2). T cells expressing iCD40 had significant baseline induction of IL2 production after OKT3 stimulation in the absence of CID (Supplementary Fig. S2). On the basis of these findings, we selected iMyD88.CD40 for testing in CAR T cells.

Generation of T Cells Expressing HER2–CARζ and iMyD88.CD40

To evaluate whether iMyD88.CD40 enhances the effector function of CAR T cells, we generated a bicistronic retroviral vector that encoded a HER2–CAR with a CD3ζ endodomain (19), a 2A sequence, and iMyD88.CD40 (HER2ζ.iCO; Fig. 1B). A HER2–CAR with a CD28ζ endodomain, which has successfully undergone clinical phase I testing (20), served as a control (HER2.CD28ζ; Fig. 1B). HER2ζ.iCO and HER2.CD28ζ T cells were generated by retroviral transduction. Mean surface CAR expression was 37.5% for HER2ζ.iCO and 43.7% for HER2.CD28ζ T cells [P = not significant (NS); $n = 6$; Fig. 1C and D]. Intracellular iCO protein expression in T cells was also confirmed by Western blot analysis (Fig. 1E). To initially demonstrate functionality of HER2ζ and iCO, HER2ζ.iCO T cells were cultured on HER2 recombinant protein–coated plates with increasing concentrations of CID. HER2ζ.iCO T cells cultured on EphA2 and HER2.CD28ζ T cells on HER2 recombinant protein–coated plates served as controls. After 24 hours, IL2 production was determined by ELISA. HER2ζ.iCO T cells stimulated with HER2 recombinant protein produced IL2 in a CID concentration–dependent manner with an EC_{50} of 0.62 nmol/L. In contrast, CID did not induce IL2 production in HER2ζ.iCO T cells simulated with EphA2 recombinant protein, nor did it increase IL2 production of HER2.CD28ζ T cells (Supplementary Fig. S3). On the basis of the determined EC_{50} of 0.62 nmol/L, all subsequent *in vitro* experiments were performed with a CID concentration of 0.5 and/or 5 nmol/L.

HER2ζ.iCO T Cells + CID Have Superior Effector Function *In Vitro* Compared with HER2.CD28ζ T Cells

To investigate the functionality of HER2ζ.iCO T cells, we first analyzed the ability of T cells to expand in the presence of antigen and CID using a repeat stimulation assay. T cells were cocultured with HER2-positive (LM7, A549, and MDA-MB-468 genetically modified to express human HER2; MDA-hHER2) or HER2-negative (MDA-MB-468) cells in the absence or presence of 0.5 and 5 nmol/L CID. Every 7 days, live T cells were counted before being restimulated with fresh tumor cells ± CID. NT and HER2.CD28ζ T cells served as controls. In the presence of 0.5 or 5 nmol/L CID, HER2ζ.iCO T cells expanded up to 10,000-fold after 4 stimulations with MDA-hHER2 and up to 1,000-fold with A549 or LM7 (Fig. 2A). In contrast, HER2.CD28ζ T cells expanded only up to 10-fold and failed to expand after the third stimulation. HER2ζ.iCO T cells did not significantly expand in the presence of HER2-positive cells without CID, or in the presence of HER2-negative cells with CID, demonstrating that expansion of HER2ζ.iCO T cells is dependent on both HER2 antigen and the presence of CID.

To evaluate whether improved expansion of HER2ζ.iCO T cells in the presence of CID was due to increased cytokine production, we determined the concentration of Th1 (IFNγ, GMCSF, TNFα, IL2) and Th2 (IL4, IL5, IL6, IL10, IL13) cytokines by multiplex analysis 48 hours after each stimulation. In the presence of CID, after each stimulation HER2ζ.iCO T cells produced high levels of Th1 cytokines (>1,000 pg/mL for 12/12 stimulations for IFNγ and GM-CSF; 11/12 for TNFα; 10/12 for IL2; Fig. 2B and C; Supplementary Fig. S4A and S4B). HER2ζ.iCO T cells + CID also produced Th2 cytokines after each stimulation, although the concentrations were less for IL4, IL5, IL6, and IL10 (IL4 and IL10: ≤100 pg/mL for 11/12 stimulations; IL5: 100–1,000 pg/mL for 6/12 stimulations; for IL6, 4/12 stimulations). HER2ζ.iCO T cells without CID consistently produced cytokines only after the first stimulation, whereas HER2.CD28ζ T cells produced cytokines after both the first and second stimulations.

To investigate the cytolytic ability of HER2ζ.iCO T cells, we utilized a repeat stimulation assay in which T cells were restimulated weekly with HER2-positive tumor cells at increasing T-cell to tumor cell ratios. After the first stimulation, HER2ζ.iCO T cells were able to kill HER2-positive LM7 and A549 cells in the presence of CID and at lower T cell to tumor cell ratios compared with HER2.CD28ζ T cells (Fig. 3). HER2ζ.iCO T cells + CID were able to kill both LM7 and A549 cells for up to four stimulations, whereas HER2.CD28ζ T cells failed to kill LM7 and A549 cells after the second restimulation. Similar to T-cell expansion and cytokine

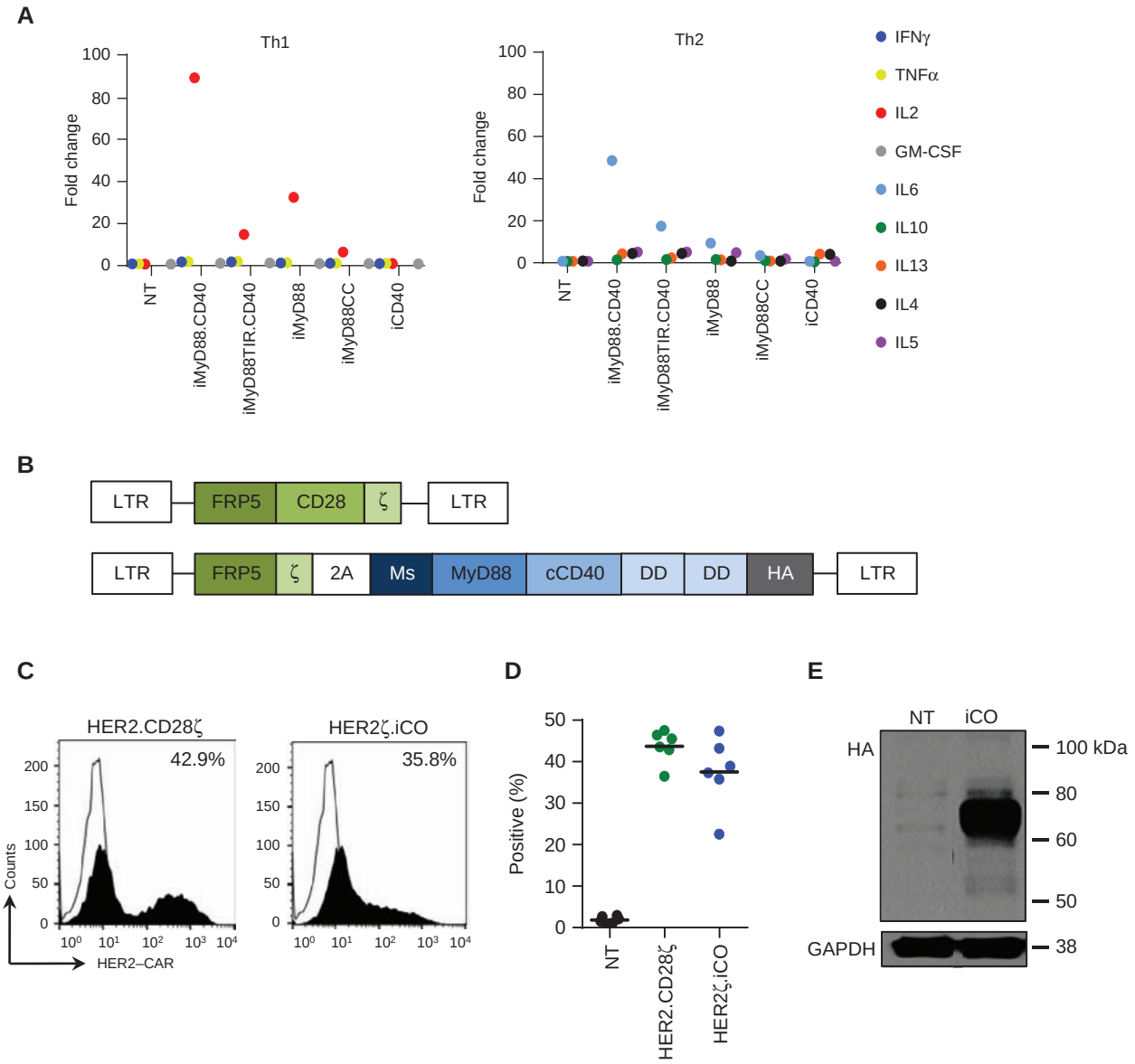

Figure 1. Generation of T cells expressing HER2-CAR and MyD88/CD40-based iCO molecule. **A,** To determine which iCO molecule to test in CAR T cells, T cells expressing iCO molecules were activated with OKT3 (0.25 μg) with or without CID (50 nmol/L), and cell culture supernatants were collected after 24 hours. Cytokine production was measured by a cytokine multiplex analysis, and data were plotted as fold change between OKT3 and OKT3 + CID conditions ($n = 3$–4 donors). **B,** Scheme of retroviral vectors encoding HER2.CD28ζ and HER2ζ.iCO. (Ms, myristoylation-targeting sequence; DD, dimerizing domain; HA, HA-epitope). **C** and **D,** HER2-CAR surface expression was determined on T cells 5 days post-transduction by FACS analysis. Representative example (open line, NT T cells; filled-in line, transduced T cells) and summary plot. CAR expression was analyzed by gating on live cells. **E,** iCO expression in T cells was confirmed by Western blot analysis using an HA antibody.

production, the ability of HER2ζ.iCO T cells to sequentially kill tumor cells was CID dependent.

To confirm that a functional CAR is required for the superior effector function of HER2ζ.iCO T cells, we generated a HER2ζ.iCO-encoding retroviral vector in which the CD3ζ signaling domain of HER2-CARζ was inactivated by replacing the six tyrosines in the ITAMs of CD3ζ with phenylalanine (HER2Δ.iCO). Although there was no difference between HER2-CAR expression of HER2Δ.iCO and HER2ζ.iCO T cells, HER2Δ.iCO T cells (i) did not produce IL2; (ii) had no cytolytic activity; and (iii) did not expand in the presence HER2-positive cells + CID (Supplementary Fig. S5A–S5D). Thus, the effector function of HER2ζ.iCO T cells is dependent on a functional CAR.

MyD88 and CD40 Signaling in HER2ζ.iCO T Cells Does Not Induce PD-1 Expression

To characterize the phenotype of HER2ζ.iCO T cells *in vitro*, we performed phenotypic analysis before and after stimulation (CD4, CD8, CCR7, CD45RO, PD-1, TIM3, LAG3). Prior to stimulation, HER2ζ.iCO and HER2.CD28ζ T cells contained similar percentages of T_N ($CCR7^+CD45RO^-$),

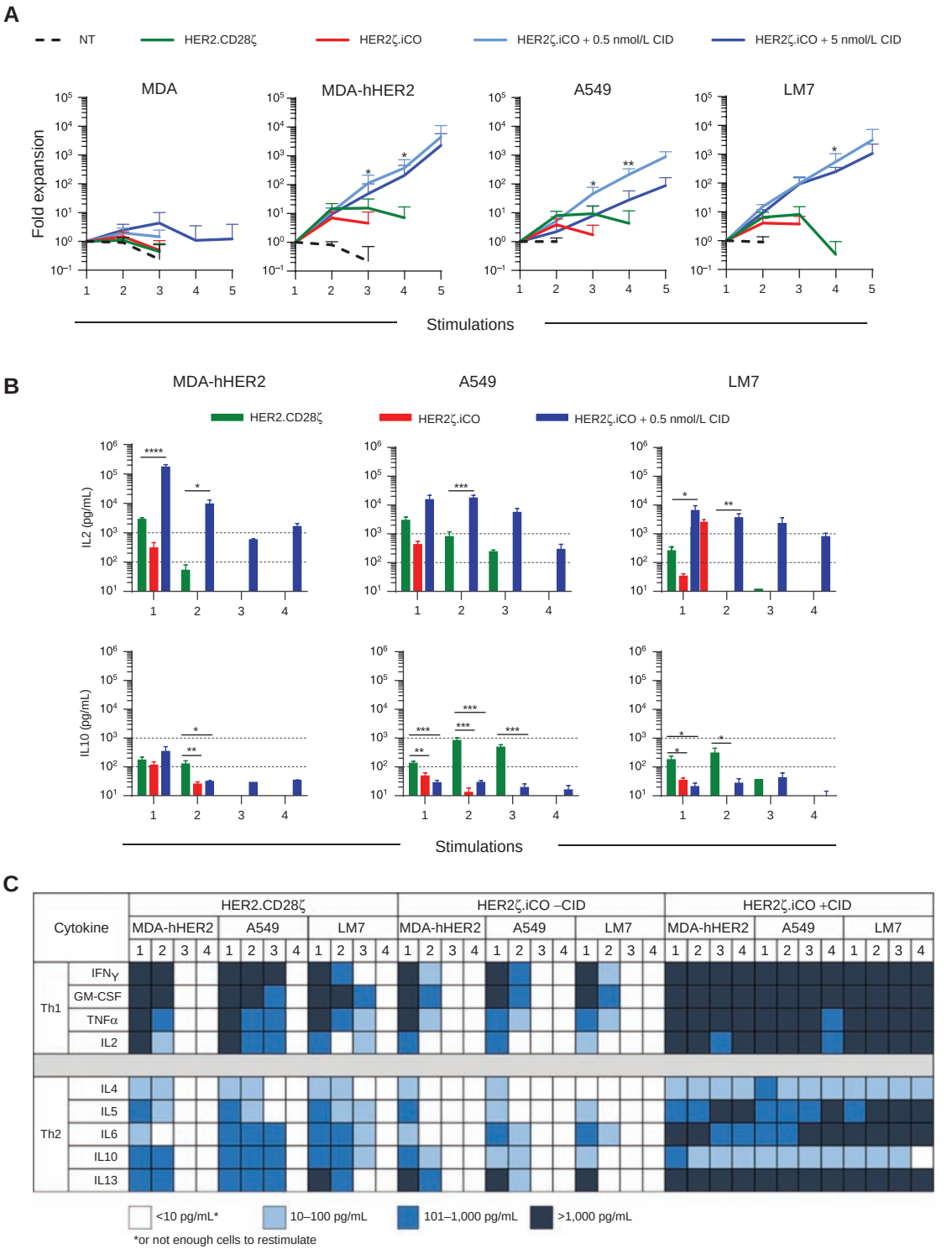

Figure 2. iCO activation enhances expansion and proinflammatory cytokine secretion of HER2ζ.iCO T cells. **A,** To measure expansion, HER2ζ.iCO T cells were cocultured with tumor cells with or without CID (0.5 or 5 nmol/L) at a 1:1 ratio and restimulated with fresh tumor cells ±CID at a 1:1 ratio every 7 days. NT and HER2.CD28ζ T cells served a control. Live T cells were counted after 7 days with Trypan blue exclusion dye (mean + SD; $n = 3$–5 donors; one-way ANOVA). **B** and **C,** To measure cytokine production, HER2ζ.iCO T cells with or without CID (0.5 nmol/L) and HER2.CD28ζ T cells were repeatedly stimulated as described above. Cell culture supernatant was harvested 48 hours after each stimulation, and multiplex assay was used to determine cytokine production (mean + SD; $n = 3$ donors; one-way ANOVA). All statistical analysis was done compared with HER2.CD28ζ T cells (*, $P < 0.05$; **, $P < 0.01$; ***, $P < 0.001$; ****, $P < 0.0001$).

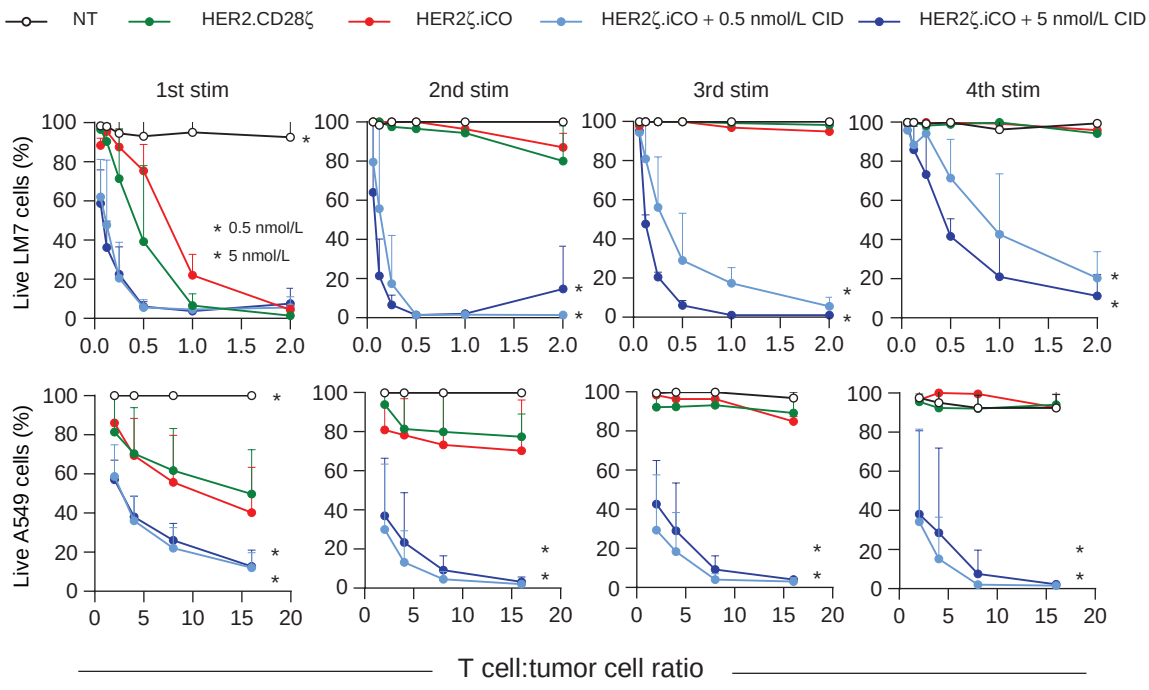

Figure 3. iCO activation enhances cytolytic activity of HER2ζ.iCO T-cells. HER2ζ.iCO T cells were cocultured with tumor cells at increasing T cell to tumor cell ratios with or without CID (0.5 or 5 nmol/L) and after 7 days (LM7 cells) or 3 days (A549 cells), T cells were harvested and replated with fresh tumor cells ±CID. NT and HER2.CD28ζ T cells served as controls. Live tumor cells were quantified after each stimulation (stim) using MTS tetrazolium compound (mean + SD; triplicates of $n = 3$; two-way ANOVA; *, $P < 0.0001$).

T_{EM} ($CCR7^-CD45RO^+$), T_{CM} ($CCR7^+CD45RO^+$), and T_{EMRA} ($CCR7^-CD45RO^-$) T-cell subsets (Supplementary Fig. S6A). After the first stimulation with HER2-positive cells the T_{CM} subset decreased in HER2.CD28ζ and HER2ζ.iCO + CID T cells. However, the decrease was lower in $CD8^+$ and $CD4^+$ HER2ζ.iCO T cells + CID [$CD4^+$ HER2.CD28ζ: 9.8% vs. $CD4^+$ HER2ζ.iCO: 18.7% (P = NS); $CD8^+$ HER2.CD28ζ: 8.1% vs. $CD8^+$ HER2ζ.iCO: 30.9% ($P < 0.01$)]. No difference in T-cell subsets was observed after the second stimulation (Supplementary Fig. S6B and S6C). PD-1 expression of HER2ζ.iCO T cells + CID was significantly lower after the second stimulation on $CD4^+$ and $CD8^+$ HER2ζ.iCO T cells compared with HER2.CD28ζ T cells (Fig. 4; Supplementary Fig. S7). Without CID, PD-1 expression of HER2ζ.iCO T cells was similar to HER2.CD28ζ T cells. There were no significant differences in the cell-surface expression of TIM3 between HER2ζ.iCO ± CID and HER2.CD28ζ T cells. $CD4^+$ and $CD8^+$ HER2ζ.iCO T cells + CID expressed significantly higher levels of LAG3 compared with $CD4^+$ and $CD8^+$ HER2.CD28ζ T cells after the first stimulation; however, LAG3 expression was significantly decreased in $CD4^+$ HER2ζ.iCO T cells + CID after the second stimulation in comparison with $CD4^+$ HER2.CD28ζ T cells.

HER2ζ.iCO T Cells Have Superior Antitumor Activity in the LM7 Xenograft Model

To evaluate the antitumor activity of HER2ζ.iCO T cells *in vivo*, we used the metastatic osteosarcoma LM7 xenograft mouse model (21). NSG mice were injected intravenously with 2×10^6 LM7.eGFP.ffluc cells, and on day 28, mice received one intravenous dose of 3×10^5 HER2ζ.iCO, HER2Δ.iCO, or HER2.CD28ζ T cells. Half of the mice of the HER2ζ.iCO T-cell group also received one intraperitoneal injection of CID, whereas the other half received one intraperitoneal injection of vehicle control. Mice treated with HER2Δ.iCO T cells also received one intraperitoneal injection of CID. Compared with injection of vehicle control, CID enhanced the antitumor activity of HER2ζ.iCO T cells with complete resolution of tumors in 7 of 9 mice within 4 weeks of T-cell injection as judged by bioluminescence imaging (Fig. 5A–C). HER2Δ.iCO T cells + CID had no antitumor activity, indicating that the antitumor activity is dependent on the presence of both signal 1 (HER2) and signal 2 (CID). HER2ζ.iCO T cells + CID also had significantly greater antitumor activity than HER2.CD28ζ T cells, resulting in a significant overall survival benefit ($P < 0.05$; Fig. 5D). Subsets of recurring tumors were analyzed for HER2 expression at the time of euthanasia, and tumors of 3 of 3 mice expressed HER2, indicating that immune escape was not a mechanism for tumor recurrence (Supplementary Fig. S8).

We next evaluated the *in vivo* expansion and persistence of HER2ζ.iCO T cells. NSG mice were injected with unmodified LM7 cells, and on day 28, 3×10^5 eGFP.ffluc-expressing HER2ζ.iCO or HER2.CD28ζ T cells were injected intravenously. Half of the mice from the HER2ζ.iCO T-cell group also received one intraperitoneal injection of CID, whereas the other half received one intraperitoneal injection of vehicle control. There was no significant difference in expansion and persistence of HER2.CD28ζ and HER2ζ.iCO T cells + CID; however, HER2.CD28ζ T cells were mainly located in the

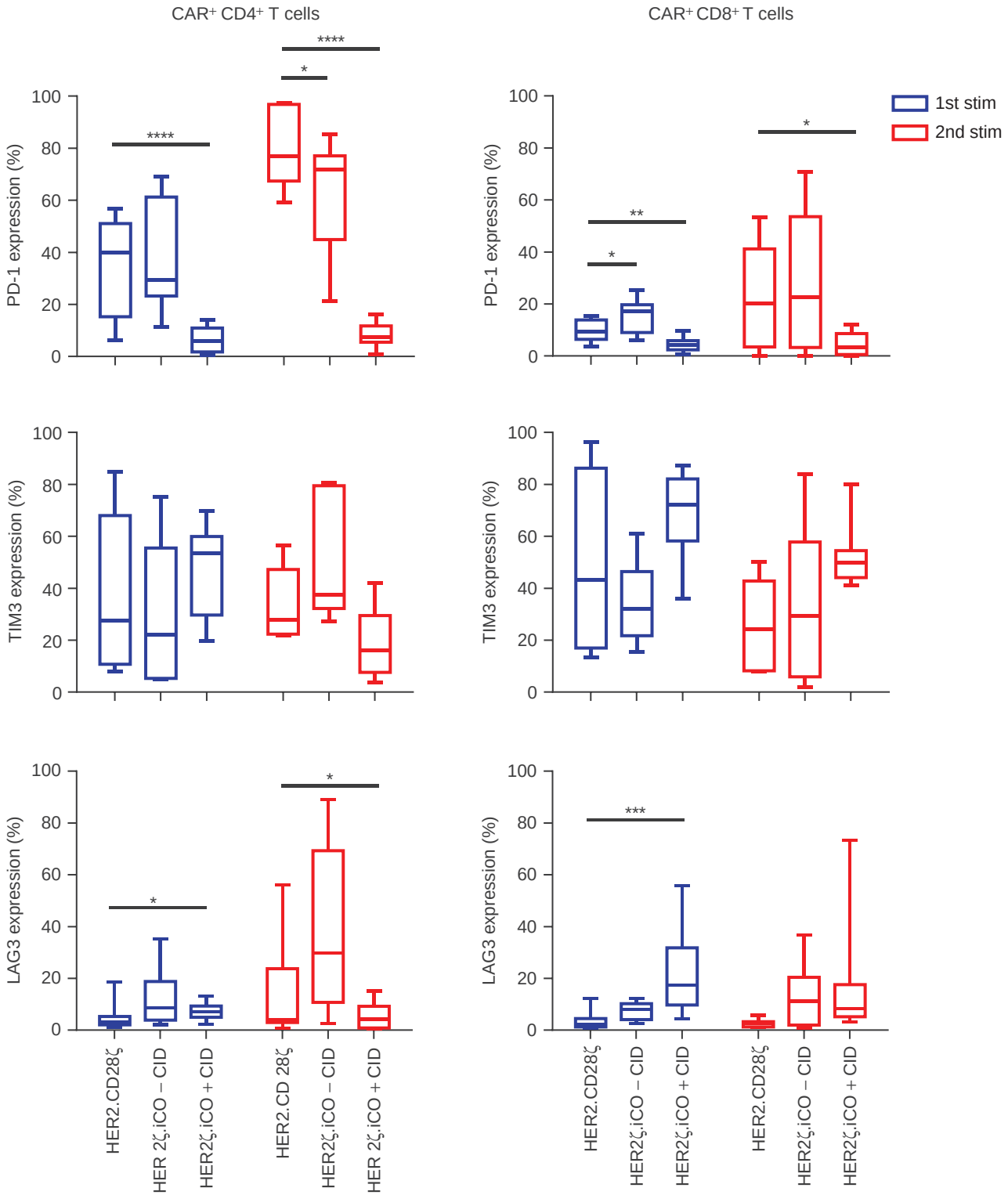

Figure 4. HER2ζ.iCO T cells have reduced PD-1 surface expression after repeat stimulations. CD4+ and CD8+ CAR T cells were analyzed for PD-1, TIM3, and LAG3 surface expression 7 days after stimulation (stim) with HER2-positive cells with or without CID (0.5 and 5 nmol/L data combined). HER2.CD28ζ T cells served as control (mean; $n = 3$ donors; 2–3 HER2-positive cell lines per donor; one-way ANOVA). All statistical analysis was done compared with HER2.CD28ζ T cells (*, $P < 0.05$; **, $P < 0.01$; ***, $P < 0.001$; ****, $P < 0.0001$).

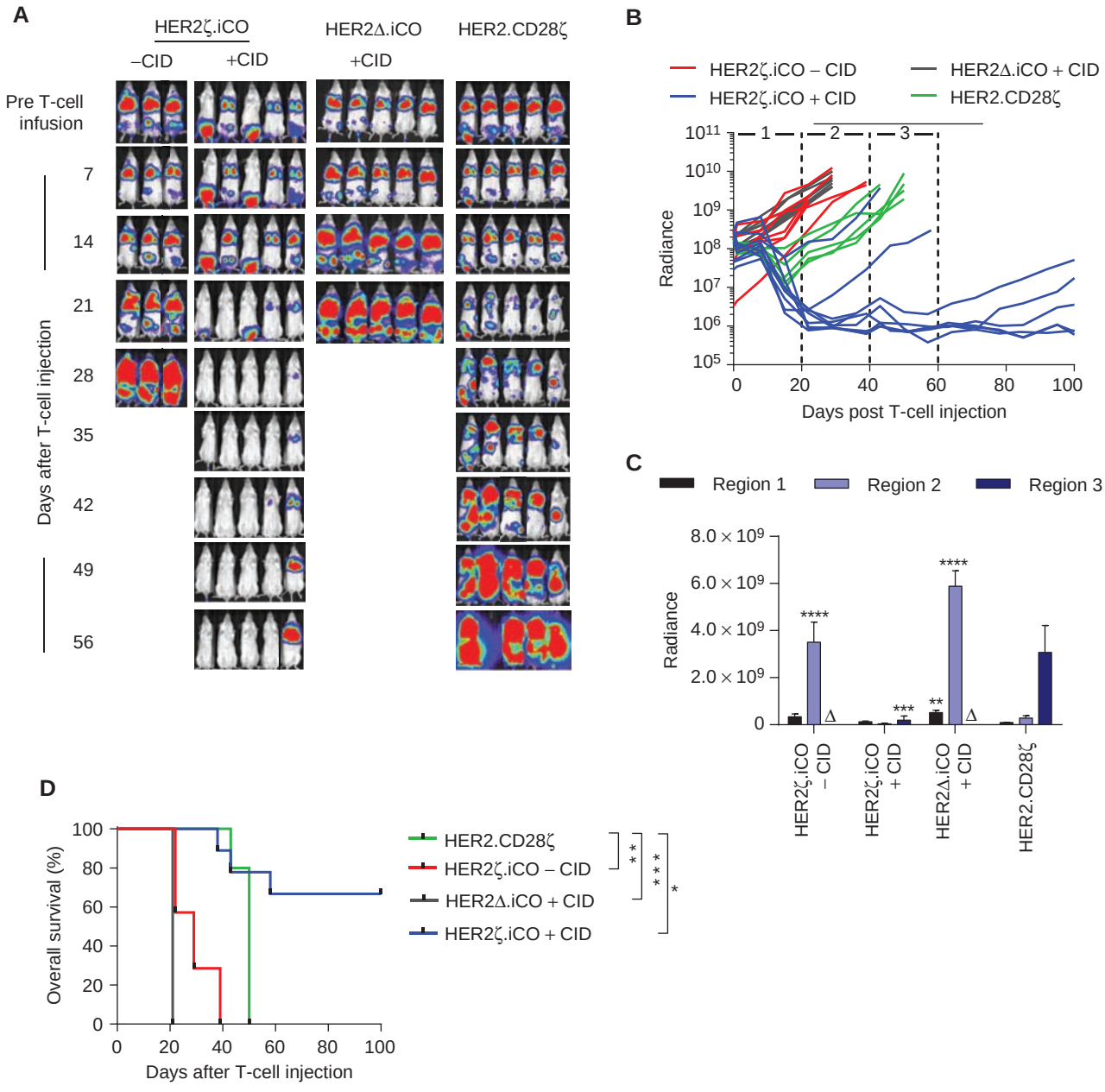

Figure 5. HER2ζ.iCO T cells have superior antitumor capability *in vivo* compared with HER2.CD28ζ T cells. LM7.eGFP.ffluc cells (2×10^6) were injected into NSG mice intravenously. On day 28, 3×10^5 HER2ζ.iCO, HER2Δ.iCO, or HER2.CD28ζ T cells were injected intravenously. Mice were injected with one dose of CID (100 μg) or vehicle control intraperitoneally (–CID) on the same day of T-cell injection. Bioluminescence imaging was used to follow tumor growth in mice. **A,** Images of representative animals are shown. **B,** Bioluminescence signal (radiance = photons/sec/cm^2/sr). Region 1: <20 days, region 2: 20≤ to <40 days; region 3: 60≤ to <60 days after T-cell injection. **C,** Pooled bioluminescence data for each region (mean + SEM; Δ: all mice euthanized; **, $P < 0.01$; ***, $P < 0.001$; ****, $P < 0.0001$; one-way ANOVA). **D,** Kaplan–Meier survival curve of HER2ζ.iCO T cells + vehicle control ($n = 7$), HER2ζ.iCO T cells + CID ($n = 9$), HER2Δ.iCO T cells + CID ($n = 10$) and HER2.CD28ζ T cells ($n = 5$; *, $P < 0.05$; **, $P < 0.01$; ***, $P < 0.001$; log-rank test). All statistical analysis was done compared with HER2.CD28ζ T cells.

lung, whereas HER2ζ.iCO T cells were present throughout the body (Fig. 6A and B). HER2ζ.iCO T cells without CID did not expand or persist.

To provide additional insight in regards to the phenotype of HER2.CD28ζ and HER2ζ.iCO T cells + CID *in vivo*, mice were injected with LM7 cells and on day 28 received one dose of 3×10^5 HER2ζ.iCO T cells + CID or HER2.CD28ζ CAR T cells. On day 10 after T-cell injection, mice were euthanized, and the frequency and phenotype of human T cells was determined by FACS analysis in the lungs and spleen. Human T cells were detected only in the lung. Although HER2ζ.iCO T cells + CID retained their CD4/CD8 ratio *in vivo*, there was a significant decrease in the percentage of CD4$^+$ T cells for HER2.CD28ζ CAR T cells. No differences were observed

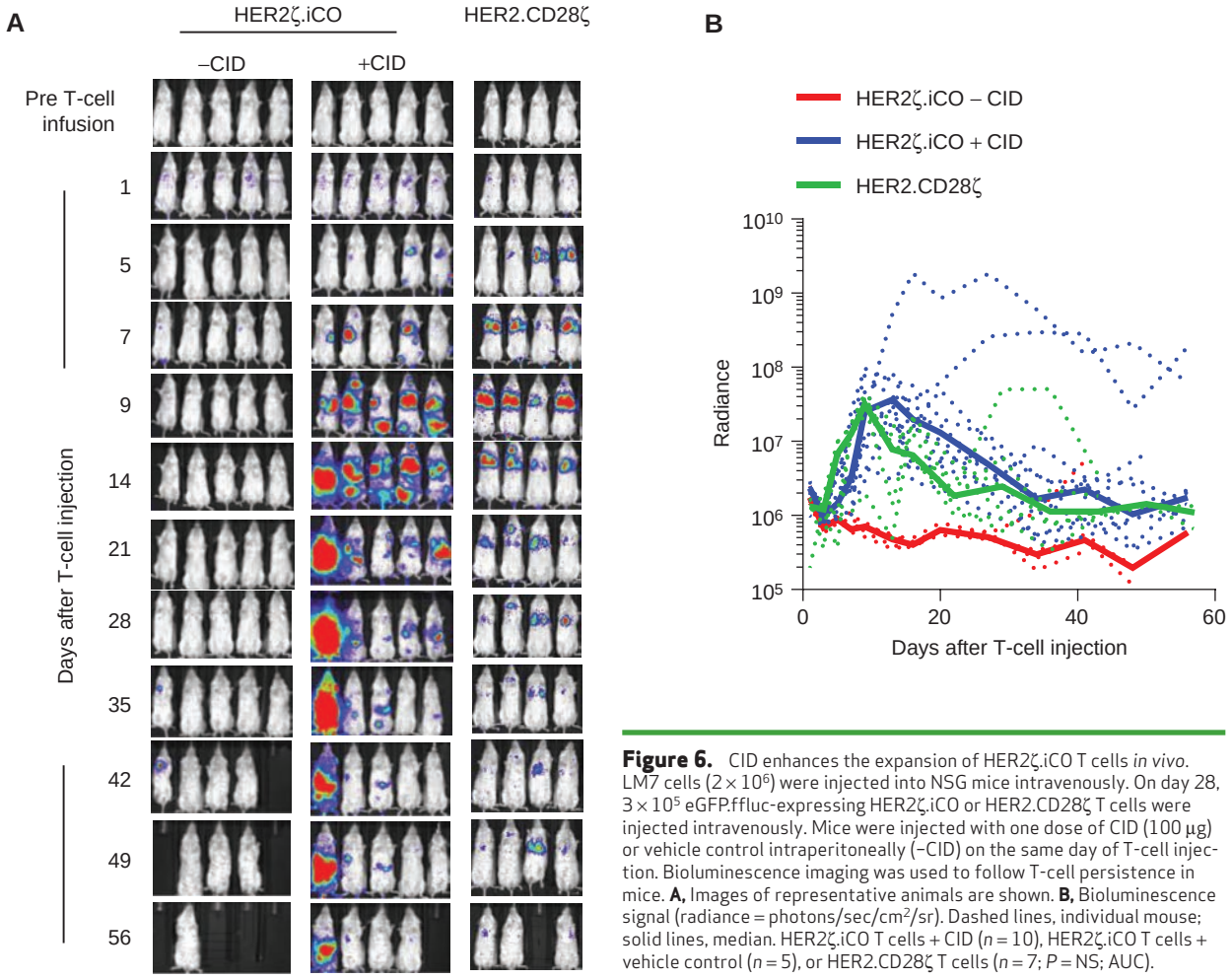

Figure 6. CID enhances the expansion of HER2ζ.iCO T cells *in vivo*. LM7 cells (2×10^6) were injected into NSG mice intravenously. On day 28, 3×10^5 eGFP.ffluc-expressing HER2ζ.iCO or HER2.CD28ζ T cells were injected intravenously. Mice were injected with one dose of CID (100 μg) or vehicle control intraperitoneally (–CID) on the same day of T-cell injection. Bioluminescence imaging was used to follow T-cell persistence in mice. **A,** Images of representative animals are shown. **B,** Bioluminescence signal (radiance = photons/sec/cm^2/sr). Dashed lines, individual mouse; solid lines, median. HER2ζ.iCO T cells + CID ($n = 10$), HER2ζ.iCO T cells + vehicle control ($n = 5$), or HER2.CD28ζ T cells ($n = 7$; P = NS; AUC).

in regard to CCR7, CD45RO, LAG3, and PD-1 expression between both groups (Supplementary Fig. S9).

Multiple Doses of CID Improve the Antitumor Activity of HER2ζ.iCO T Cells *In Vivo*

To evaluate whether multiple doses of CID enhance the antitumor activity of HER2ζ.iCO T cells, we used the aggressive non–small cell lung cancer A549 xenograft model (22). NSG mice were injected with 2×10^6 A549.eGFP.ffluc cells, and on day 7 mice received 3×10^5 HER2.CD28ζ or HER2ζ.iCO T cells + CID or vehicle control. Of the mice that received CID, one group received additional doses of CID on days 13, 35, and 48 after T-cell injection. Multiple doses of CID induced superior antitumor activity of HER2ζ.iCO T cells compared with HER2ζ.iCO T cells ± one dose of CID, and HER2.CD28ζ T-cells (Fig. 7A–C), resulting in a significant survival advantage (Fig. 7D). Subsets of mice that had received HER2ζ.iCO T cells and either vehicle control or 4 doses of CID underwent routine histologic examinations at the time of euthanasia. Although mice treated with HER2ζ.iCO T cells with vehicle control had tumors in the lung and long bones, mice treated with HER2ζ.iCO T cells and CIDx4 had tumors only in the pelvis, confirming our bioluminescence imaging results (Supplementary Fig. S10). To investigate why the majority of animals had died of progressive tumors in their pelvis, we determined chemokine secretion by A549 cells using a human chemokine array, and chemokine receptor expression of HER2ζ.iCO T cells by FACS analysis. CXCL5 was the most abundant chemokine expressed by A549 cells; however, less than 20% of HER2ζ.iCO T cells expressed the corresponding chemokine receptor, CXCR2 (Supplementary Fig. S11). Thus, limited T-cell homing to tumor sites could have contributed to this therapeutic failure.

DISCUSSION

We show here that inducible activation of MyD88 and CD40 signaling pathways in HER2ζ.iCO T cells enhances their effector function as judged by T-cell proliferation, cytokine production, and ability to kill target cells sequentially. HER2ζ.iCO T cells + CID had superior effector function *in vitro* and improved antitumor activity *in vivo* compared with HER2.CD28ζ T cells. In addition, we demonstrate that the antitumor activity of HER2ζ.iCO T cells can be modulated *in vivo* by repeat CID injections.

Several approaches are being developed to modulate CAR T-cell activity with a second molecule. For example, T cells expressing CARs with ectodomains that consist of avidin or

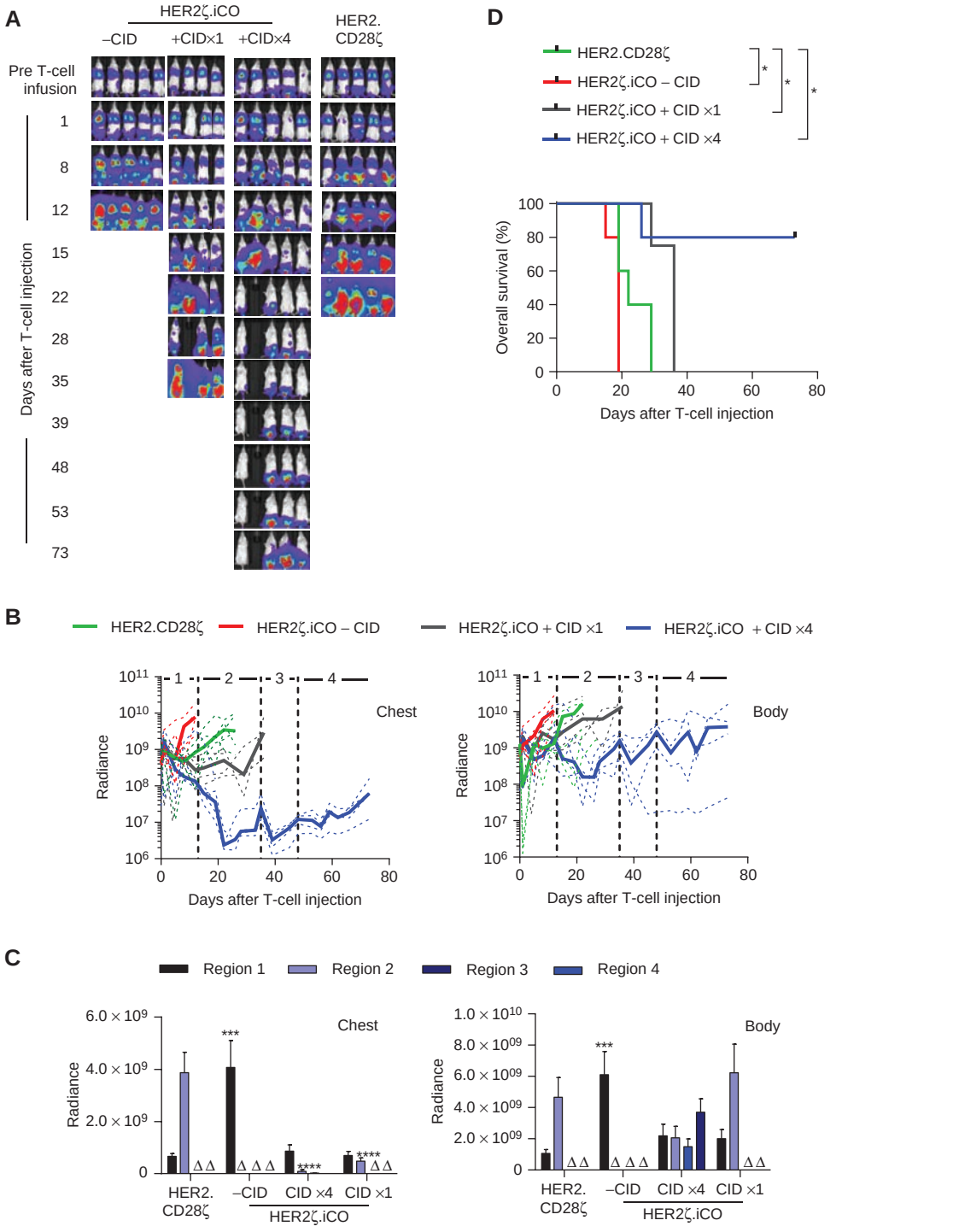

Figure 7. Multiple doses of CID improve the antitumor activity of HER2ζ.iCO T cells *in vivo*. A549.eGFP.ffluc cells (2×10^6) were injected into NSG mice intravenously. On day 7, 3×10^5 HER2ζ.iCO or HER2.CD28ζ T cells were injected intravenously. Mice were injected with one dose of CID (100 μg) or vehicle control intraperitoneally (–CID) on the same day of T-cell injection. One group of HER2ζ.iCO + CID T-cell mice received three additional doses of CID intraperitoneally (days 13, 35, and 48 after T-cell injection). Bioluminescence imaging was used to follow tumor growth in mice. **A,** Images of representative animals are shown. **B,** Bioluminescence signal (radiance = photons/sec/cm^2/sr). Dashed lines, individual mouse; solid lines, median. Regions of graph correspond to CID injections as follows: region 1, T-cell and CID injection #1; region 2, CID injection #2; region 3, CID injection #3; region 4, CID injection #4. **C,** Pooled bioluminescence data for each region (mean + SEM; Δ, all mice euthanized; ***, $P < 0.001$; ****, $P < 0.0001$; one-way ANOVA). **D,** Kaplan–Meier survival curve of HER2ζ.iCO T cells + CIDx1 ($n = 4$), HER2ζ.iCO T cells + CIDx4 ($n = 5$), HER2ζ.iCO T cells + vehicle control ($n = 5$), or HER2.CD28ζ T cells ($n = 5$; *, $P < 0.05$; log-rank test). All statistical analysis was done compared with HER2.CD28ζ T cells.

recognize FITC can be redirected to tumor cells with biotin- or FITC-labeled antibodies (23, 24). In addition, CARs have been designed in which the antigen-binding domain can be dimerized with signaling domains using CID (25). Although these approaches can modulate CAR T-cell activity post infusion *in vivo*, they provide ζ-activation (signal 1) and costimulation (signal 2) simultaneously. This might not be optimal, as physiologic signals 1 and 2 are separated in T cells (26). In addition, the majority of CARs have utilized CD28 and/or TNFR family members (CD27, 41BB, OX40) as costimulatory endodomains (27). To closely mimic physiologic T-cell activation and potentially augment signal 2 with alternative costimulatory molecules, we explored whether the effector function of CAR T cells expressing an inducible MyD88/CD40–based iCO molecule can be modulated by CID.

We initially determined whether activation of TIR-domain deleted MyD88 and/or CD40 significantly enhances T-cell cytokine production after CD3 simulation. MyD88 activation increased IL2 production 7- to 32-fold, and MyD88 and CD40 activation 89-fold. Reintroducing the TIR domain into iMyD88.CD40, a protein–protein interaction domain shown to interact with PI3K and induce downstream signaling and IL2 production, surprisingly reduced IL2 production 6-fold despite previous reports (11). MyD88 activation also induced an increase in IL6 production (up to 48-fold for iMyD88.CD40), whereas CD40 activation alone did not. Although high levels of IL6 have been associated with cytokine release syndrome after CD19–CAR T-cell infusions (28, 29), we selected the iCO molecule that induced the highest amount of IL2 production for testing in CAR T cells, given their limited activity in solid tumors (30).

HER2ζ.iCO and HER2.CD28ζ T cells were generated by retroviral transduction. Although the percent of CAR-positive cells was similar, the mean fluorescence intensity of CAR expression for HER2ζ.iCO T cells was lower. As observed by others, this is most likely due to differences in the transmembrane domain between both CARs (ζ vs. CD28; ref. 31). To test the functionality of HER2ζ.iCO T cells, we initially performed experiments with optimal amounts of plate-bound recombinant HER2 protein. Although we observed a clear difference between a CID dose of 0.5 and 5 nmol/L, this was not consistently observed when we performed coculture assays with HER2-positive tumor cells. Several factors most likely contributed to the observed differences, including the use of cell lines that express HER2 at low levels, and potentially, inhibitory molecules (e.g., PD-L1) expressed by tumor cells.

After the first challenge with cancer cells, there were only minor differences between HER2ζ.iCO T cells + CID and HER2.CD28ζ T cells in regard to T-cell proliferation, cytokine production, and cytolytic activity. After the second stimulation (day 7), however, HER2.CD28ζ T cells had decreased effector function, and on day 14, their effector function was completely eroded. HER2ζ.iCO T cells + CID, in particular the $CD4^+$ T-cell subset, expressed lower levels of PD-1 after the second stimulation compared with HER2.CD28ζ T cells. As the tumor cells used in our experiment expressed PD-L1 in the presence of IFNγ (Supplementary Fig. S12), reduced expression of PD-1 could have contributed to the improved effector function of HER2ζ.iCO T cells. However, *in vivo,* we did not observe a difference in PD-1 expression between HER2ζ.iCO T cells + CID and HER2.CD28ζ T cells 10 days after T-cell injection. Clearly, besides a careful longitudinal analysis of PD-1 expression on the cell surface of adoptively transferred T cells *in vivo*, additional mechanistic studies are needed. For example, the IFN regulator factor 7 (IRF7) pathway has recently been shown to be critical for optimal CAR T-cell function. This pathway is not activated in T cells expressing CD28ζ CARs (32). Interestingly, MyD88 associates with IRF7, and the MyD88–IRF7 signaling complex is critical for a high level of IFN production (33).

Separating signal 1 from signal 2 might also have contributed to the superior effector function of HER2ζ.iCO T cells, especially because CARs with costimulatory endodomains are prone to baseline, tonic signaling (34). To investigate this further, we generated HER2.CD28ζ.iCO (Supplementary Fig. S13), and their effector function was compared ± CID with HER2ζ.iCO T cells *ex vivo* using serial restimulation assays. Expansion, cytokine production, and sequential killing were assessed. Similar to HER2ζ.iCO T cells, addition of CID significantly improved the effector function of HER2.CD28ζ.iCO T cells. Direct comparison of HER2ζ.iCO and HER2.CD28ζ.iCO T cells in the presence of CID showed no significant difference in regard to expansion of and cytokine production by T cells (Supplementary Fig. S14). However, for one of the tested cell lines, HER2.CD28ζ.iCO T cells + CID showed improved cytolytic activity in sequential killing assays (Supplementary Fig. S15). Thus, inducible costimulation can also improve the effector function of T cells that express a CAR with a CD28 costimulatory endodomain. Additional studies are needed to extend our findings, especially to T cells that express CARs with other costimulatory endodomains, including 4-1BB, which has been reported to induce less tonic signaling than CD28 (34).

Although HER2ζ.iCO T cells + CID had greater antitumor activity in the LM7 model compared with HER2.CD28ζ T cells, we did not observe a significant difference in HER2.CD28ζ and HER2ζ.iCO + CID T-cell expansion *in vivo*. However, HER2.CD28ζ T cells expanded only in the lung, the major site of disease after tail-vein injection of LM7 cells (35). In contrast, HER2ζ.iCO T cells in the presence of CID also expanded at other anatomic sites within mice that mirrored extrapulmonary sites of disease as judged by bioluminescent imaging. As the majority of T cells after tail-vein injection traffic to the lung, our findings could be explained by the inability of HER2.CD28ζ T cells to migrate to extrapulmonary sites of disease upon activation by tumors within lungs. In addition, it is possible that low numbers of HER2.CD28ζ T cells initially trafficked to extrapulmonary sites but might not have been able to expand, given their limited ability to expand in repeat stimulation assays *in vitro*. Studies are planned to differentiate between both scenarios.

In vivo, HER2ζ.iCO T cells + CID had potent antitumor activity in the LM7 model. However, 4 of 9 mice had late recurrences. One mouse with a recurring tumor was euthanized to determine HER2 expression of the tumor, and, as it was positive, the other 3 mice received a second dose of CID 100 days after the initial HER2ζ.iCO T-cell injection. Two of three tumors decreased in size as judged by bioluminescence imaging (Supplementary Fig. S16). Taken together with our findings that 4 doses of CID conferred superior antitumor

activity in the A549 model, these results suggest that CID can effectively modulate CAR T-cell function *in vivo*. One limitation of our study is that we used xenograft models to study the effector function of HER2ζ.iCO T cells *in vivo*, which do not recapitulate the immunosuppressive tumor microenvironment. On the basis of our encouraging findings, further evaluation of our approach in immunocompetent animal models is warranted.

AP20187, the CID used in this study, has an estimated half-life of 7 hours in mice (36), which is similar to the half-life (5 hours) of clinical grade AP1903 in humans (37). Despite its short half-life, one dose of CID or multiple doses separated by 13 to 22 days significantly enhanced the antitumor activity of HER2ζ.iCO T cells. These results strongly suggest that intermittent costimulation is sufficient to enhance the effector function of CAR T cells *in vivo*. In fact, this pattern mimics physiologic costimulation, during which T cells do not continuously encounter APCs that express costimulatory molecules (26). Being able to provide intermittent costimulation should also greatly enhance the safety of HER2ζ.iCO T cells. If safety issues should arise, suicide gene switches that do not rely on CID are readily available, including transgenic expression of truncated EGFR in combination with the FDA-approved monoclonal cetuximab (38), or an iC9 suicide gene, which is dimerized with rapamycin (39).

In conclusion, we demonstrate that the effector function of HER2ζ T cells can be enhanced by expressing iMyD88.CD40. In the presence of CID, HER2ζ.iCO T cells had superior effector function and antitumor activity than HER2.CD28ζ T cells in two solid tumor xenograft models, and their antitumor activity could be modulated by intermittent CID dosing. Thus, inducible activation of MyD88 and CD40 in CAR T cells has the potential to improve current CAR T-cell therapy approaches for solid tumors. In addition, our devised strategy should be applicable to non–CAR-based T-cell therapies.

METHODS

Tumor Cell Lines

The breast cancer cell line, MDA-MB-468, and the non–small cell lung cancer cell line, A549, were purchased in 2003 (MDA-MB-468) and 2008 (A549) from ATCC. The metastatic osteosarcoma cell line, LM7, was kindly provided by Dr. Eugenie Kleinerman (MD Anderson Cancer Center, Houston, TX) in 2011. The MDA-MB-468 cell line expressing human HER2 (MDA-hHER2) was generated as described previously (40). All adherent tumor cell lines were grown in DMEM (Invitrogen) containing 10% heat-inactivated FCS and 1% GlutaMax (Life Technologies) and cultured at 37°C in 5% CO_2. Cell lines were cell authenticated (The Characterized Cell Line Core Facility, MD Anderson Cancer Center, Houston, TX) and routinely checked for *Mycoplasma* by the MycoAlert Mycoplasma Detection Kit (Lonza).

Generation of Retroviral Vectors

The generation of HER2 CARs with transmembrane and signaling endodomains of the T-cell receptor ζ-chain (first generation) and human CD28 transmembrane and CD28ζ signaling endodomains (second generation) has been described previously (19, 20). The original iCO construct containing both MyD88 and CD40 was described previously (9). All iCO constructs outlined in Supplementary Fig. S1 were synthesized by Thermo Fisher Scientific and cloned into a pSFG retroviral vector containing an IRES and mOrange. The HER2ζ.iCO construct was generated by combining the first-generation HER2–CAR with the iCO construct containing both the MyD88 adaptor protein (lacking the TIR domain) and the intracellular CD40 signaling domain. The two genes were linked together using a 2A sequence. The sequence of all cloned constructs was confirmed by sequencing (Seqwright).

Transduction of Human T Cells

RD114-pseudotyped viral particles encoding iCO or HER2ζ.iCO were produced by transient transfection of 293T cells as described previously (20). GALV-pseudotyped viral particles encoding the HER2.CD28ζ CAR were collected from a PG13 producer cell line. Human peripheral blood mononuclear cells (PBMC) from healthy donors were obtained under a Baylor College of Medicine Institutional Review Board (IRB)–approved protocol, after informed consent was obtained in accordance with the Declaration of Helsinki. T cells from PBMCs were activated by stimulation on OKT3 (CRL-8001, ATCC) and anti-CD28 (Becton Dickinson) coated nontissue culture-treated 24-well plates. Recombinant human IL7 (10 ng/μL, PeproTech) and IL15 (5 ng/μL, PeproTech) were added to cultures on day 2, and the following day, cells were transduced with retroviral particles immobilized on RetroNectin (Clontech Laboratories) coated plates. T cells were maintained and expanded in the presence of IL7 and IL15 (41).

Flow Cytometry

A FACSCanto II flow cytometer (BD Biosciences) was used to acquire immunofluorescence data, which was analyzed with FlowJo software Version X.0.7 (Tree Star). Forward- and side-scatter gating was used to discriminate live cells from dead cells. HER2–CAR expression was analyzed as described previously (20, 42). Surface expression on T cells of various markers was determined using the following antibodies: CD4 (Beckman Coulter), CD8 (Beckman Coulter), CD45RO (BD Biosciences), CCR7 (R&D, Minneapolis, MN), PD-1 (BD Biosciences), TIM3 (BioLegend), and LAG3 (R&D Systems).

Western Blot Analysis

Cells were dissociated with PBS + 3 mmol/L ethylenediaminetetraacetic acid and lysed in a buffer containing 50 mmol/L Tris, 150 mmol/L NaCl, 5 mmol/L ethylenediaminetetraacetic acid, 1% Triton X-100 (all from Sigma), and protease inhibitors (Thermo Fisher Scientific). Protein concentrations were determined using a Bio-Rad protein assay (Bio-Rad) with BSA as the standard. Samples were denatured in Laemmli buffer (Bio-Rad) with βME (2-mercaptoethanol, Bio-Rad) at 95°C for 5 minutes. Cell lysates (5 μg/lane) were run on a 10% SDS polyacrylamide gel and transferred to nitrocellulose membranes (Bio-Rad). Membranes were blocked with 5% BSA (for phosphorylated proteins) or 5% milk in Tris-buffered saline + 0.1% Tween-20 (all from Sigma) and then probed with either anti–phospho-IKKα/β (Cell Signaling Technology), anti-IKKα (Cell Signaling Technology), or anti-HA (Bethyl Laboratories, Inc.). Anti-rabbit IgG, HRP-linked or anti-mouse IgG, HRP-linked was used as secondary antibody (Cell Signaling Technology). GAPDH or β-actin (Santa Cruz Biotechnology) was used as a housekeeping gene. Blots were developed using SuperSignal West Dura Extended Duration Substrate (Thermo Fisher Scientific) and exposed to GeneMate Blue Basic Autoradiography Film (BioExpress).

Repeat Stimulation and MTS Assay

Tumor cells (2×10^3 per well) were plated with various ratios of effector T cells in complete RPMI with or without CID (B/B Homodimerizer, equivalent to AP20187; Clontech Laboratories, Inc.) and incubated for 3 days (A549 cells) or 7 days (LM7 cells) at 37°C in 5% CO_2. T cells were then harvested and replated with fresh 2×10^3 tumor cells per well and incubated for another stimulation for 3 or 7 days at 37°C in 5% CO_2. Repeated stimulations were done up to 4 weeks. To assess live tumor cells after each stimulation, tumor

cells were incubated with an MTS tetrazolium [3-(4,5-dimethylthiazol-2-yl)-5-(3-carboxymethoxyphenyl)-2-(4-sulfophenyl)-2H-tetrazolium] compound (CellTiter96 AQ_{ueous} One solution cell proliferation assay, Promega) for 2 hours at 37°C in 5% CO_2, and absorbance was read at 492 nm. Tumor cells with media served as control, and wells with media alone served as a blank. Live tumor cell percentage was calculated as follows: (average absorbance − blank absorbance)/(tumor cell alone absorbance − blank absorbance) × 100. Assays were performed in triplicate in 96-well plates.

Analysis of Cytokine Production

Genetically modified T cells or NT T cells were either activated with OKT3 (0.25 μg) or cocultured with HER2-negative or HER2-positive human cell lines at a 1:1 effector-to-target ratio in a 24-well plate. CID (B/B Homodimerizer, equivalent to AP20187; Clontech Laboratories, Inc.) at various concentrations was added immediately after coculture. After 48 hours of incubation, culture supernatants were harvested, and cytokine production was measured by a human cytokine/chemokine multiplex assay (EMD Millipore) as per the manufacturer's instructions.

Systemic Murine Xenograft Tumor Model

Eight- to 10-week-old female NSG (NOD.Cg-Prkdc^{scid} Il2rg^{tm1Wjl}/SzJ, The Jackson Laboratory) mice were injected intravenously with 2×10^6 LM7.eGFP.ffLuc cells or A549.eGFP.ffluc (in 200 μL PBS), and tumors were allowed to establish for 28 or 7 days, respectively. Animals were then treated with one tail-vein injection of effector cells (3×10^5 in 200 μL PBS) and one intraperitoneal injection of CID (100 μg/mouse) or vehicle control. CID (Clontech Laboratories, Inc.) was prepared with PEG-400 and Tween as per the manufacturers' instructions. A mixture of ethanol, PEG-400, and Tween was used as vehicle control. Additional CID injections were given intraperitoneally at various time points. To assess T-cell persistence, mice were injected intravenously with 2×10^6 unmodified LM7 cells, and tumors were allowed to establish for 28 days before 3×10^5 CAR T cells modified to express eGFP.ffluc were injected intravenously. Mice treated with effector cells and injected intraperitoneally with vehicle control served as controls. Mice were euthanized when they met euthanasia criteria (weight loss, signs of distress) in accordance with the Center for Comparative Medicine at Baylor College of Medicine (Houston, TX). Pathologic analysis of murine tissue and tumors was performed at the Comparative Pathology Laboratory at Baylor College of Medicine.

Bioluminescence Imaging

Isoflurane-anesthetized animals were imaged using the IVIS system (IVIS, Xenogen Corp.) 10 to 15 minutes after 150 mg/kg D-luciferin (Xenogen) per mouse was injected intraperitoneally. The photons emitted from the luciferase-expressing tumor cells were quantified using Living Image software 64 (Caliper Life Sciences). A pseudocolor image representing light intensity (blue least intense and red most intense) was generated and superimposed over the grayscale reference image. A constant region of interest was drawn over the whole animal excluding the tail, and the intensity of the signal was measured as total p/s/cm^2/sr. After effector T-cell injections, animals were imaged every day for T-cell persistence experiments or once a week for tumor cell tracking. Mice were euthanized when the tumor radiance was greater than 5×10^9 or when they met euthanasia criteria (weight loss, signs of distress) in accordance with the Center for Comparative Medicine at Baylor College of Medicine.

Statistical Analysis

All experiments were performed at least in duplicate. For comparison between two groups, two-tailed *t* test was used. For comparisons of three or more groups, the values were analyzed by ANOVA with Bonferroni post-test. To determine EC_{50}, data were normalized and nonlinear regression was performed. Survival determined from the time of T-cell injection was analyzed by the Kaplan–Meier method and by the log-rank test. Bioluminescence imaging data were analyzed using either ANOVA, *t* test, or AUC.

Study Approval

Human PBMCs from healthy donors were obtained under a Baylor College of Medicine IRB-approved protocol, after informed consent was obtained in accordance with the Declaration of Helsinki. Human PBMCs were isolated from healthy donors. All animal experiments followed a protocol approved by the Baylor College of Medicine Institutional Animal Care and Use Committee.

Disclosure of Potential Conflicts of Interest

D.M. Spencer has ownership interest (including patents) in Bellicum Pharmaceuticals. S. Gottschalk has patent applications in the fields of T-cell and/or gene therapy for cancer and is a consultant/advisory board member for Merrimack. No potential conflicts of interest were disclosed by the other authors.

Authors' Contributions

Conception and design: M. Mata, S. Gottschalk
Development of methodology: M. Mata, S. Gottschalk
Acquisition of data (provided animals, acquired and managed patients, provided facilities, etc.): M. Mata, P. Nguyen, G. Krenciute
Analysis and interpretation of data (e.g., statistical analysis, biostatistics, computational analysis): M. Mata, G. Krenciute, D.M. Spencer, S. Gottschalk
Writing, review, and/or revision of the manuscript: M. Mata, G. Krenciute, D.M. Spencer, S. Gottschalk
Administrative, technical, or material support (i.e., reporting or organizing data, constructing databases): M. Mata, C. Gerken, P. Nguyen, S. Gottschalk
Study supervision: S. Gottschalk
Other (development of iMC): D.M. Spencer

Acknowledgments

We thank Dr. Roger Price at the Comparative Pathology Laboratory at Baylor College of Medicine for his assistance with the pathologic analysis of murine tissue, and Catherine Gillespie for editing the manuscript.

Grant Support

M. Mata received NIH grant 5T32HL092332 and S. Gottschalk received NIH grant 1R01CA173750 and CRPIT grant RP101335 to support this work.

The costs of publication of this article were defrayed in part by the payment of page charges. This article must therefore be hereby marked *advertisement* in accordance with 18 U.S.C. Section 1734 solely to indicate this fact.

Received March 10, 2017; revised July 1, 2017; accepted August 7, 2017; published OnlineFirst August 11, 2017.

REFERENCES

1. Park JH, Geyer MB, Brentjens RJ. CD19-targeted CAR T-cell therapeutics for hematologic malignancies: interpreting clinical outcomes to date. Blood 2016;127:3312–20.
2. Beatty GL, O'Hara M. Chimeric antigen receptor-modified T cells for the treatment of solid tumors: Defining the challenges and next steps. Pharmacol Ther 2016;166:30–9.

3. Kershaw MH, Wang G, Westwood JA, Pachynski RK, Tiffany HL, Marincola FM, et al. Redirecting migration of T cells to chemokine secreted from tumors by genetic modification with CXCR2. Hum Gene Ther 2002;13:1971–80.
4. Cui Y, Zhang H, Meadors J, Poon R, Guimond M, Mackall CL. Harnessing the physiology of lymphopenia to support adoptive immunotherapy in lymphoreplete hosts. Blood 2009;114:3831–40.
5. Newick K, Moon E, Albelda SM. Chimeric antigen receptor T-cell therapy for solid tumors. Mol Ther Oncolytics 2016;3:16006.
6. Morgan RA, Yang JC, Kitano M, Dudley ME, Laurencot CM, Rosenberg SA. Case report of a serious adverse event following the administration of T cells transduced with a chimeric antigen receptor recognizing ERBB2. Mol Ther 2010;18:843–51.
7. Lamers CH, Sleijfer S, van SS, van EP, van KB, Groot C, et al. Treatment of metastatic renal cell carcinoma with CAIX CAR-engineered T cells: clinical evaluation and management of on-target toxicity. Mol Ther 2013;21:904–12.
8. Di Stasi A, Tey SK, Dotti G, Fujita Y, Kennedy-Nasser A, Martinez C, et al. Inducible apoptosis as a safety switch for adoptive cell therapy. N Engl J Med 2011;365:1673–83.
9. Narayanan P, Lapteva N, Seethammagari M, Levitt JM, Slawin KM, Spencer DM. A composite MyD88/CD40 switch synergistically activates mouse and human dendritic cells for enhanced antitumor efficacy. J Clin Invest 2011;121:1524–34.
10. Reynolds JM, Dong C. Toll-like receptor regulation of effector T lymphocyte function. Trends Immunol 2013;34:511–9.
11. Gelman AE, LaRosa DF, Zhang J, Walsh PT, Choi Y, Sunyer JO, et al. The adaptor molecule MyD88 activates PI-3 kinase signaling in CD4+ T cells and enables CpG oligodeoxynucleotide-mediated costimulation. Immunity 2006;25:783–93.
12. Geng D, Zheng L, Srivastava R, Asprodites N, Velasco-Gonzalez C, Davila E. When Toll-like receptor and T-cell receptor signals collide: a mechanism for enhanced CD8 T-cell effector function. Blood 2010;116:3494–504.
13. Geng D, Zheng L, Srivastava R, Velasco-Gonzalez C, Riker A, Markovic SN, et al. Amplifying TLR-MyD88 signals within tumor-specific T cells enhances antitumor activity to suboptimal levels of weakly immunogenic tumor antigens. Cancer Res 2010;70:7442–54.
14. Munroe ME, Bishop GA. A costimulatory function for T cell CD40. J Immunol 2007;178:671–82.
15. Bourgeois C, Rocha B, Tanchot C. A role for CD40 expression on CD8+ T cells in the generation of CD8+ T cell memory. Science 2002;297:2060–3.
16. Bhadra R, Gigley JP, Khan IA. Cutting edge: CD40-CD40 ligand pathway plays a critical CD8-intrinsic and -extrinsic role during rescue of exhausted CD8 T cells. J Immunol 2011;187:4421–5.
17. Rogers NJ, Jackson IM, Jordan WJ, Lombardi G, Delikouras A, Lechler RI. CD40 can costimulate human memory T cells and favors IL-10 secretion. Eur J Immunol 2003;33:1094–104.
18. Ahmed N, Brawley VS, Hegde M, Robertson C, Ghazi A, Gerken C, et al. Human epidermal growth factor receptor 2 (HER2) -specific chimeric antigen receptor-modified T cells for the immunotherapy of HER2-positive sarcoma. J Clin Oncol 2015;33:1688–96.
19. Ahmed N, Ratnayake M, Savoldo B, Perlaky L, Dotti G, Wels WS, et al. Regression of experimental medulloblastoma following transfer of HER2-specific T cells. Cancer Res 2007;67:5957–64.
20. Ahmed N, Salsman VS, Yvon E, Louis CU, Perlaky L, Wels WS, et al. Immunotherapy for osteosarcoma: genetic modification of T cells overcomes low levels of tumor antigen expression. Mol Ther 2009;17:1779–87.
21. Jia SF, Worth LL, Kleinerman ES. A nude mouse model of human osteosarcoma lung metastases for evaluating new therapeutic strategies. Clin Exp Metastasis 1999;17:501–6.
22. Kakarla S, Chow KK, Mata M, Shaffer DR, Song XT, Wu MF, et al. Antitumor effects of chimeric receptor engineered human T cells directed to tumor stroma. Mol Ther 2013;21:1611–20.
23. Rodgers DT, Mazagova M, Hampton EN, Cao Y, Ramadoss NS, Hardy IR, et al. Switch-mediated activation and retargeting of CAR-T cells for B-cell malignancies. Proc Natl Acad Sci U S A 2016;113:E459–68.
24. Urbanska K, Lanitis E, Poussin M, Lynn RC, Gavin BP, Kelderman S, et al. A universal strategy for adoptive immunotherapy of cancer through use of a novel T-cell antigen receptor. Cancer Res 2012;72:1844–52.
25. Wu CY, Roybal KT, Puchner EM, Onuffer J, Lim WA. Remote control of therapeutic T cells through a small molecule-gated chimeric receptor. Science 2015;350:aab4077.
26. Chen L, Flies DB. Molecular mechanisms of T cell co-stimulation and co-inhibition. Nat Rev Immunol 2013;13:227–42.
27. Sadelain M, Brentjens R, Riviere I. The promise and potential pitfalls of chimeric antigen receptors. Curr Opin Immunol 2009;21:215–23.
28. Maude SL, Frey N, Shaw PA, Aplenc R, Barrett DM, Bunin NJ, et al. Chimeric antigen receptor T cells for sustained remissions in leukemia. N Engl J Med 2014;371:1507–17.
29. Lee DW, Kochenderfer JN, Stetler-Stevenson M, Cui YK, Delbrook C, Feldman SA, et al. T cells expressing CD19 chimeric antigen receptors for acute lymphoblastic leukaemia in children and young adults: a phase 1 dose-escalation trial. Lancet 2015;385:517–28.
30. Rosenberg SA. IL-2: the first effective immunotherapy for human cancer. J Immunol 2014;192:5451–8.
31. Savoldo B, Ramos CA, Liu E, Mims MP, Keating MJ, Carrum G, et al. CD28 costimulation improves expansion and persistence of chimeric antigen receptor-modified T cells in lymphoma patients. J Clin Invest 2011;121:1822–6.
32. Zhao Z, Condomines M, van der Stegen SJ, Perna F, Kloss CC, Gunset G, et al. Structural design of engineered costimulation determines tumor rejection kinetics and persistence of CAR T cells. Cancer Cell 2015;28:415–28.
33. Ning S, Pagano JS, Barber GN. IRF7: activation, regulation, modification and function. Genes Immun 2011;12:399–414.
34. Long AH, Haso WM, Shern JF, Wanhainen KM, Murgai M, Ingaramo M, et al. 4-1BB costimulation ameliorates T cell exhaustion induced by tonic signaling of chimeric antigen receptors. Nat Med 2015;21:581–90.
35. Duan X, Jia SF, Zhou Z, Langley RR, Bolontrade MF, Kleinerman ES. Association of alphavbeta3 integrin expression with the metastatic potential and migratory and chemotactic ability of human osteosarcoma cells. Clin Exp Metastasis 2004;21:747–53.
36. Welm BE, Freeman KW, Chen M, Contreras A, Spencer DM, Rosen JM. Inducible dimerization of FGFR1: development of a mouse model to analyze progressive transformation of the mammary gland. J Cell Biol 2002;157:703–14.
37. Iuliucci JD, Oliver SD, Morley S, Ward C, Ward J, Dalgarno D, et al. Intravenous safety and pharmacokinetics of a novel dimerizer drug, AP1903, in healthy volunteers. J Clin Pharmacol 2001;41:870–9.
38. Wang X, Chang WC, Wong CW, Colcher D, Sherman M, Ostberg JR, et al. A transgene-encoded cell surface polypeptide for selection, in vivo tracking, and ablation of engineered cells. Blood 2011;118:1255–63.
39. Duong MT, Lu A, Collinson-Pautz MR, Brandt ME, Slawin KM, Yvon ES, et al. Dual-switch GoCAR-T cells: dual molecular switches to control activation and elimination of CAR-T cells to target CD123 (+) cancer in vivo. Mol Ther 2017;25:252–3.
40. Mata M, Vera JF, Gerken C, Rooney CM, Miller T, Pfent C, et al. Toward immunotherapy with redirected T cells in a large animal model: ex vivo activation, expansion, and genetic modification of canine T cells. J Immunother 2014;37:407–15.
41. Xu Y, Zhang M, Ramos CA, Durett A, Liu E, Dakhova O, et al. Closely related T-memory stem cells correlate with in vivo expansion of CAR.CD19-T cells and are preserved by IL-7 and IL-15. Blood 2014;123:3750–9.
42. Chow KK, Naik S, Kakarla S, Brawley VS, Shaffer DR, Yi Z, et al. T cells redirected to EphA2 for the immunotherapy of glioblastoma. Mol Ther 2013;21:629–37.